Dale P. Bentz,[1] *Edward J. Garboczi,*[1] *and Eric S. Lagergren*[2]

Multi-Scale Microstructural Modeling of Concrete Diffusivity: Identification of Significant Varibles

Authorized Reprint from Journal of Cement, Concrete, and Aggregates June 1998

REFERENCE: Bentz, D. P., Garboczi, E. J., and Lagergren, E. S., **"Multi-Scale Microstructural Modeling of Concrete Diffusivity: Identification of Significant Variables,"** *Cement, Concrete, and Aggregates,* CCAGDP, Vol. 20, No. 1, June 1998, pp. 129–139.

ABSTRACT: The ability to predict the expected chloride diffusivity of a concrete based on its mixture proportions and field-curing conditions would be of great benefit both in predicting service life of the concrete and in developing durability-based design codes. Here, a multi-scale microstructural computer model is applied to computing the chloride diffusivities of concretes with various mixture proportions and projected degrees of hydration. A fractional factorial experimental design has been implemented to study the effects in the model of seven major variables: water-to-cement (*W/C*) ratio, degree of hydration, aggregate volume fraction, coarse aggregate particle size distribution, fine aggregate particle size distribution, interfacial transition zone thickness, and air content. Based on this experimental design, *W/C* ratio, degree of hydration, and aggregate volume fraction have been identified as the three major variables influencing concrete diffusivity in the model. Following identification of the significant variables, a response surface design has been executed and least squares regression used to develop a simple equation for predicting chloride ion diffusivity in concrete based on these three parameters. This simple equation essentially summarizes the complicated simulations involved in computing the model response. Finally, simulations have been conducted to examine the extent of the surface layer in cast-in-place concrete, where the local aggregate volume fraction near the surface is less than that to be found in the bulk of the concrete.

KEYWORDS: concrete diffusivity, durability, experimental design, interfacial transition zone, microstructure, modeling, performance prediction

One of the critical properties controlling the service life of concrete structures is the resistance the concrete provides to the diffusive ingress of deleterious species such as chloride and sulfate ions (Clifton and Knab 1989). A priori prediction of the chloride diffusivity of a concrete based on its mixture proportions and expected curing is needed to predict accurately its service life in its expected service environment and to allow the development of durability-based (in addition to the current strength-based) design codes. In fact, specifications are already being issued that contain quite restrictive chloride diffusivity limits to meet a 100-year service life requirement (Hooton 1995).

In this research, microstructural modeling techniques are applied to the a priori prediction of chloride ion diffusion coefficients for conventional ($0.25 < W/C < 0.75$) saturated concretes. Diffusion/sorption in partially saturated concrete, important in many field exposures, is not addressed in this study. In addition, we are considering only chloride ion diffusion under steady-state conditions, as the effects of binding of the chlorides are beyond the scope of the present study.

Because of the wide range of feature sizes in concrete, from nanometer-sized pores to centimeter-sized aggregates, it is difficult to represent concurrently all of these structural features in a single microstructural model. However, multi-scale modeling techniques may offer one solution to this restriction (Bentz et al. 1995a, 1997). In this approach, properties computed at one scale, micrometers for instance, are input into a model that encompasses a higher scale, such as millimeters. Here, microstructural models for (a) cement paste surrounding a single aggregate with a resolution of micrometers, and for (b) a representative volume of concrete on the order of 20 cm^3 in volume and containing hundreds of thousands of aggregate particles are employed. These two microstructural models are interconnected along with computational techniques for computing the relative diffusivity or relative conductivity of a three-dimensional microstructure to compute the diffusivity of a representative volume of concrete, as has been demonstrated previously for mortars (Bentz et al. 1997).

To determine which mixture proportion and curing parameters most influence the diffusivity of a concrete, a statistically designed computer experiment is conducted. Because we wish to consider seven variables at each of two levels, a fractional factorial experimental design is used to reduce the number of computer experiments required from 128 (2^7) to 16, while still obtaining information on all of the main and some of the second-order interaction effects (Box et al. 1978). Once the most significant variables have been identified, a response surface design is executed to better determine the effects of the "major" variables on diffusivity. Based on the results of this design, an equation relating diffusivity to material parameters is developed to approach our goal of the a priori prediction of concrete diffusivity. This equation essentially summarizes, in a simple analytical form, the complicated computations based on the multi-scale models.

Microstructural Models and Computational Techniques

Cement Paste Surrounding a Single Aggregate

The cement, specifically tricalcium silicate, hydration model used in this research has been described in detail elsewhere (Bentz and Garboczi 1991a, 1992a) so that only the salient features will be outlined here. The cement powder to be modeled is represented by non-overlapping digitized spheres following the particle size distribution (PSD) measured on actual cement samples. In this

[1] Chemical engineer and physicist, respectively, Building and Fire Research Laboratory, National Institute of Standards and Technology, Gaithersburg, MD 20899.
[2] Mathematical statistician, Information Technology Laboratory, National Institute of Standards and Technology, Gaithersburg, MD 20899.

study, we have employed the PSDs given by Van Breugel (1991) to examine cements with median particle diameters of 10, 20, and 30 μm. To minimize finite size effects, periodic boundaries are used during particle placement, such that a particle that extends outside of one face of our 3-D computational volume is completed (wrapped) into the opposite side of the system. In these simulations, each pixel element represents 1 μm^3 in volume and the total system size including a single flat plate aggregate is either 450 by 220 by 220 or 600 by 220 by 220 pixels. As shown in Fig. 1, the thickness of the single aggregate is adjusted so that in the computational cube, the appropriate ratio of "interfacial zone" (within the interfacial transition zone (ITZ) thickness) to "bulk" (outside the ITZ thickness) cement paste is obtained, as determined using the concrete microstructure model described below. The cement particles are placed in order of size from largest to smallest at random locations in the 3-D microstructure such that they do not overlap one another or the aggregate particle.

After initial particle placement, a simple cellular automaton model is used to model the hydration reactions between tricalcium silicate and water (Bentz et al. 1994). Cement pixels in contact with water dissolve at random, diffuse within the pore space, and react to form calcium hydroxide crystals in the pore space and calcium silicate hydrate gel (C-S-H) on the surfaces of the original cement particles and previously deposited C-S-H.

For these studies, the aggregate is considered inert and does not participate in the hydration reactions. After the user-specified volume fraction of the initial cement has reacted, known as the degree of hydration, the microstructure can be quantified by determining the capillary porosity present as a function of distance from the aggregate surface. Initially, after particle placement, the interfacial transition zone region contains a higher *W/C* ratio (more porosity) than the bulk paste due to the inefficient packing of the cement particles (the so-called "wall effect"). During hydration, the porosity is reduced throughout, but still remains higher in the ITZ regions. Thus, these regions will typically have a higher diffusivity than the bulk paste regions. Once porosity has been quantified, relative diffusivity (D/D_0) as a function of distance from the aggregate surface x can be estimated using the relationship established by Garboczi and Bentz (1992):

$$\frac{D}{D_0}(x) = 0.001 + 0.07 \cdot \phi(x)^2 + 1.8 \cdot H(\phi(x) - 0.18) \cdot (\phi(x) - 0.18)^2 \quad (1)$$

where relative diffusivity is defined as the ratio of the diffusivity of ions in the material of interest relative to their value in bulk water, $\phi(x)$ is the porosity fraction at a distance x, and H is the Heaviside function having a value of 1 when $\phi > 0.18$ and a value of 0 otherwise. The value of 0.18 indicates the capillary porosity at which the capillary pore space becomes depercolated due to hydration (Powers 1959; Garboczi and Bentz 1992).

Concrete Microstructure Model

For modeling concrete, the computational volume, typically between 8 cm^3 and 27 cm^3, is filled with hard spheres, representing aggregates, each surrounded by a constant thickness soft shell, representing the interfacial transition zone (Winslow et al. 1994). Thus, we are assuming that the ITZ thickness is not a function of the aggregate size, but is rather controlled by the median size of the much smaller cement particles (Bentz et al. 1992b). Here, we are ignoring any effects of bleeding that would tend to locally augment the interfacial transition zone thickness. Once again, the aggregates are placed into the computational volume in order from largest to smallest in size and periodic boundaries are employed. While the hard core aggregates may not overlap one another, the

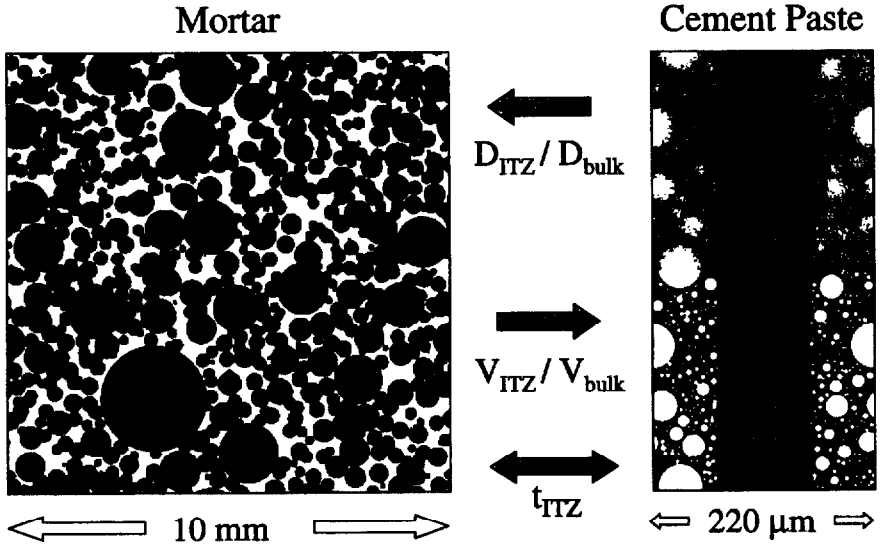

FIG. 1—*Linkages between microstructure models for mortar/concrete and cement paste for predicting diffusivity of mortar or concrete. In the mortar model (left), inclusions are grey, ITZ regions are black, and bulk paste is white. In the cement paste model, cement particles are white, water-filled porosity is black, and the flat rectangular aggregate is grey. In the hydrated image (upper right), calcium hydroxide is dark grey and calcium silicate hydrate gel is light grey. The parameters and arrows (center) indicate the flow of information between the models.*

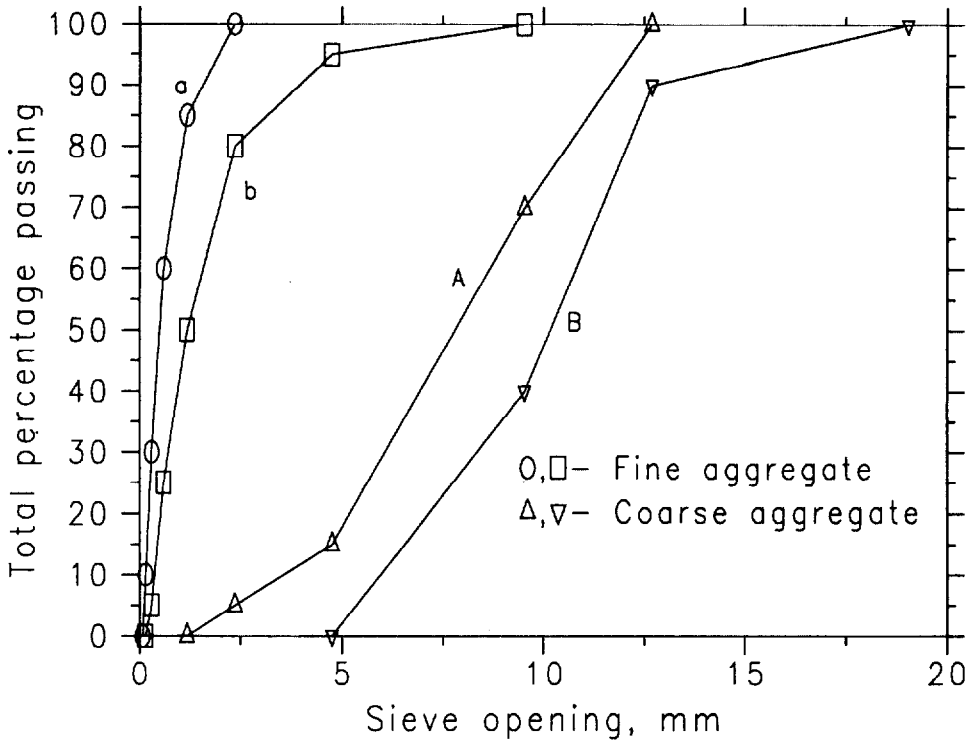

FIG. 2—*Limiting coarse and fine aggregate particle size distributions used in computer experiments.*

soft shell interfacial transition zones are free to overlap one another and partially overlap another aggregate, as shown in Fig. 1. For this study, limiting (that is, extreme) PSDs for the coarse and fine aggregates were chosen based on the recommendations found in ASTM C 33 (1995). Cumulative volume fraction curves for the limiting distributions are shown in Fig. 2. For this study, the coarse aggregate was of nominal size 4.75 to 12.5 mm and the ratio of coarse to fine aggregate volume was fixed at 1.5:1. Basheer et al. (1996) have observed only a minor influence of coarse to fine aggregate volume ratio, within the range of 2:1 to 1.43:1, on concrete permeation properties.

In addition to executing simulations for systems containing only aggregates and cement paste, studies were also conducted in which air voids were introduced into the concrete. The air voids are considered equivalent to aggregate particles in terms of their effects on chloride ion diffusivity, that is, they are assigned a relative diffusivity of 0 and lead to the formation of additional ITZ regions throughout the concrete (Rashed and Williamson 1991). For this study, a fixed air void size distribution was used for all of the simulations based on a logarithmic probability density function $g(x)$ given by Snyder and Clifton (1994):

$$g(x) = \frac{\exp\left(\frac{-(\ln(x) - \ln(d_0))^2}{2\sigma^2}\right)}{\sqrt{2\pi}\sigma d_0 \exp\left[\frac{\sigma^2}{2}\right]} \quad (2)$$

where d_0 is the modal diameter and σ is the standard deviation of the logarithms, respectively. Here, this equation was used with a modal diameter of 30 μm and a standard deviation of 0.736 (giving a specific surface of 300 cm^{-1}), as in Snyder and Clifton (1994). Air voids smaller than 100 μm in diameter were not included in the model, as they are similar in size to the cement particles.

Simulation Procedure

The simulation procedure used in this study is illustrated for a mortar in Fig. 1. To begin a simulation, the cement PSD is used to establish the interfacial transition zone thickness, t_{ITZ}, assumed to be equivalent to the median cement particle diameter. Aggregate particles following the aggregate PSD of interest are placed into the concrete volume and systematic point sampling is used to determine the volume fractions of interfacial transition zone (V_{ITZ}) and bulk (V_{bulk}) paste for this choice of aggregate PSD and t_{ITZ} (Winslow et al. 1994). At this point, for the cement hydration model, the thickness of the single aggregate particle is chosen to match this ratio of V_{ITZ}/V_{bulk} for the chosen cement PSD in the cement paste model volume. Cement particles are placed into this computational volume to achieve the desired W/C ratio, and the hydration model is executed to achieve the chosen degree of hydration. The capillary porosity is then measured as a function of distance from the aggregate surface and converted to relative diffusivity values using Eq 1. These values are averaged in two subsets, those lying within t_{ITZ} of the aggregate and those in the "bulk" paste. The ratio of these two diffusivities D_{ITZ}/D_{bulk} is then used as an input into the original concrete model. Here, random walk (myopic ant) techniques are employed to estimate the diffusivity of the overall concrete system consisting of aggregates with a diffusivity of 0, bulk paste with a diffusivity of 1, and interfacial transition zones with a diffusivity of D_{ITZ}/D_{bulk}. The random walk techniques employed for this calculation have been described in detail previously (Garboczi et al. 1995; Schwartz et al. 1995). After a large number of walkers have each taken a large number of random

steps in the concrete, the relative diffusivity of the concrete D_{conc}/D_{bulk} can be calculated (Bentz et al. 1997; Garboczi et al. 1995; Schwartz et al. 1995). This value can finally be converted into an absolute chloride ion diffusivity for the concrete D_{conc} by multiplying it by D_{bulk}/D_0 determined from the cement-level microstructural model, and by D_0, the diffusion coefficient of chloride ions in bulk water, $2.0 \cdot 10^{-9}$ m^2/s (Mills and Lobo 1989). By changing the value of D_0 to correspond to that measured for the specific ion of interest, such as sulfate ions, the above techniques can be generalized to other ionic species of relevance in cement-based materials (as long as the assumption of no chemical effects such as binding and/or reactions is a reasonable one).

Experimental Design

Because of the large number of variables that could potentially influence the chloride diffusivity of a concrete, a fractional factorial experimental design was selected to identify the subset of "significant" variables (Box et al. 1978). The seven variables examined and their low and high settings are given in Table 1. The high and low settings were chosen so as to encompass the extreme values that might be encountered in field concrete. A $2^{(7-3)}$ fractional factorial experimental design was selected to examine the effects of the seven listed variables in 16 runs. Standard design generators were used to determine the variables settings for each of the 16 runs, to assure an orthogonal resolution four design. An orthogonal resolution four design is one in which the main variable effects can be estimated free and clear from all interactions. The fractional factorial design used here has the additional property that each combination of settings for any three factors occurs the same number of times.

In addition to these 16 runs, one "center point" experiment was conducted with all of the seven variable settings at their mid-range values. For the coarse and fine particle size distributions, this mid-range was selected as the halfway point between the limits specified by ASTM C 33 (1995) and shown in Fig. 2. For two of the experiments with the higher volume fraction of aggregate and containing air voids, the air void content had to be reduced slightly from 10 to 8.5 to 9% to enable placement of all of the aggregate and air void particles, which together accounted for about 84% of the overall concrete volume, a rather dense packing even for a size distribution of spherical particles.

Once the most significant variables had been determined, a response surface design was developed to provide more quantitative information on the variables effects on the chloride diffusivity of concrete. From the initial 17 runs, *W/C* ratio, degree of hydration, and volume fraction of aggregate were determined to be significant. Six additional runs were then executed by varying each of these three variables between two extreme values while holding the other two at their mid-range value. The two extreme values were selected to be twice the distance from the mid-range value as the high and low settings shown in Table 1 (for example, 0.4 and 0.8 for degree of hydration and 0.525 and 0.825 for volume fraction of aggregate). This choice of extreme values yields a response surface whose predicted values are estimated with equal precision at any fixed distance from the center point. However, for *W/C* ratio, this proved computationally impossible, so that values of 0.25 (instead of 0.15) and 0.75 were used as the two extremes. The other four variables were fixed at computationally convenient values for the additional response surface runs since they had been shown to have only negligible effects on the concrete diffusivity.

TABLE 1—*Variables and settings examined in study.*

ID	Variable	Low Setting	High Setting
1	(*W/C*)	0.3	0.6
2	Degree of hydration, α	0.5	0.7
3	Volume fraction aggregate, V_{agg}	0.60	0.75
4	Coarse aggregate PSD	A[a]	B
5	Fine aggregate PSD	a	b
6	t_{ITZ}	10 μm	30 μm
7	Air content	0%	10%

[a] Letters refer to labeled distribution curves in Fig. 2.

The response surface design allows estimation of a second-order equation. Because the chloride diffusivity of concrete varies over several orders of magnitude for the conditions examined in this study, the log of the diffusivity was used and the following equation was fitted by ordinary least squares regression (Neter et al. 1990):

$$\log_{10}D = A_0 + \sum_{i=1}^{n} A_i \cdot x_i + \sum_{i=1}^{n}\sum_{j=i+1}^{n} B_{ij} \cdot x_i \cdot x_j + \sum_{i=1}^{n} C_i \cdot x_i^2 \quad (3)$$

where n is the number of significant variables.

Results

Computation of Diffusivities

All of the computer runs executed in this study and their resultant predicted chloride diffusivity values are provided in Table 2. The diffusivities are seen to range well over two orders of magnitude, from $2.1 \cdot 10^{-13}$ to $8.18 \cdot 10^{-11}$ m^2/s. For one system, three runs using different random number seeds were conducted to examine the variability in D due to the randomness of the microstructures. The determined coefficient of variation, less than 1.5%, justified the execution of only one computer run to obtain representative results for each of the experimental conditions. Figure 3 summarizes the effects of the seven variables considered in this study on the computed concrete diffusivity. In this figure, the variables are identified by the IDs given in the first column of Table 1. For each

TABLE 2—*Parameter values and resultant chloride diffusivities.*

W/C, mass	α	V_{agg}	CA PSD	FA PSD	t_{ITZ}, μm	Air Content, vol %	D_{conc}, 10^{-12} m^2/s
0.3	0.5	0.6	A	a	10	0	2.1 (0.33)[a]
0.3	0.5	0.6	B	a	30	10	4.0 (0.60)
0.3	0.5	0.75	A	b	30	10	1.75 (0.24)
0.3	0.5	0.75	B	b	10	0	1.2 (0.079)
0.3	0.7	0.6	A	b	30	0	0.84 (−0.08)
0.3	0.7	0.6	B	b	10	10	0.44 (−0.36)
0.3	0.7	0.75	A	a	10	9	0.21 (−0.68)
0.3	0.7	0.75	B	a	30	0	0.69 (−0.16)
0.6	0.5	0.6	A	b	10	10	58.1 (1.76)
0.6	0.5	0.6	B	b	30	0	77.7 (1.89)
0.6	0.5	0.75	A	a	30	0	41. (1.61)
0.6	0.5	0.75	B	a	10	9	28.7 (1.46)
0.6	0.7	0.6	A	a	30	10	28.4 (1.45)
0.6	0.7	0.6	B	a	10	0	36.3 (1.56)
0.6	0.7	0.75	A	b	10	0	20.1 (1.30)
0.6	0.7	0.75	B	b	30	10	12.9 (1.11)
0.45	0.6	0.675	mid	mid	20	5	9.4 (0.97)
0.45	0.6	0.525	B	b	10	0	16.3 (1.21)
0.45	0.6	0.825	B	b	10	0	5.34 (0.73)
0.45	0.4	0.675	B	b	10	0	39.5 (1.6)
0.45	0.8	0.675	B	b	10	0	1.76 (0.25)
0.75	0.6	0.675	B	b	10	0	81.8 (1.91)
0.25	0.6	0.675	B	b	10	0	0.47 (−0.33)

[a] Values in parentheses indicate the $\log_{10}$ ($D_{conc} \cdot 10^{-12}$).

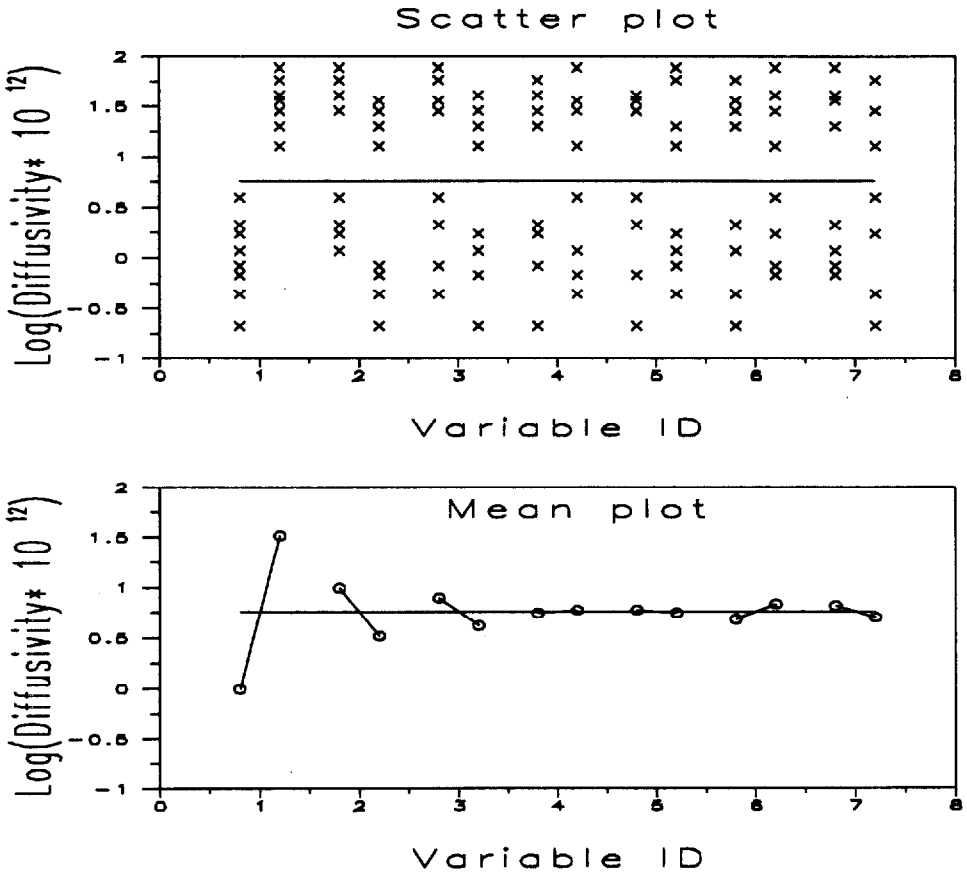

FIG. 3—*Scatter (top) and mean (bottom) plots for $\log_{10}$ of the chloride diffusivity of concrete versus the seven variables identified in Table 1.*

variable, the results obtained for the low variable setting lie to the left of the ID, while those computed for the high variable setting lie to the right of the ID. The horizontal line in each figure indicates the global mean value for the 16 runs. The scatter plot illustrates all of the data values obtained in the first 16 runs, while the mean plot shows only the mean values obtained for the eight runs with the low variable setting contrasted against the mean for the eight runs with the high setting. From the mean plot, one can observe that *W/C* ratio, degree of hydration, and volume fraction of aggregate are the most significant variables. The thickness of the interfacial transition zone and air content are less significant and the coarse and fine aggregate particle size distributions have almost no effect on the computed diffusivities.

Some insight into the effects of these variables can be gained by considering two components of the overall concrete diffusivity, the inherent diffusivity of the bulk paste portion, D_{bulk} and its attenuation/diminution by the presence of aggregates (and air voids) and their accompanying interfacial transition zones, as indicated by the value of D_{conc}/D_{bulk}. This second parameter is strongly influenced by the volume of interfacial zone paste and the ratio of D_{ITZ} to D_{bulk} (Garboczi et al. 1995; Schwartz et al. 1995). The effects of each variable on these two parameters can be summarized as follows:

W/C *Ratio*—Numerous experimental (Gautefall 1986; Page et al. 1981; Atkinson and Nickerson 1984; Halamickova et al. 1995) and computer model (Garboczi and Bentz 1992) results have indicated that a reduction in *W/C* ratio will lead to a significant reduction in diffusivity. This large reduction is only partially off-set by the fact that a decrease in *W/C* ratio does actually lead to a slight increase in the ratio of D_{conc} to D_{bulk}, as it increases the ratio D_{ITZ}/D_{bulk}, particularly at the lower degrees of hydration.

Degree of Hydration—Increasing the degree of hydration (age) is observed to both decrease the diffusivity of the bulk cement paste and also decrease the value of D_{conc}/D_{bulk}. The latter reduction is due to the fact that the porosities in the interfacial transition zone and bulk regions become closer to one another as hydration proceeds (Bentz et al. 1997) and to the reduced slope of Eq 1 at low porosities.

Volume Fraction of Aggregate—Increasing the volume fraction of aggregate creates a greater volume of ITZ cement paste, which in turn leads to a larger reduction in the *W/C* ratio of the "bulk" paste (Bentz et al. 1997). Thus, an increased volume fraction of aggregate will result in a reduction in the value of D_{bulk}. The effect of the volume fraction of aggregate on the value of D_{conc}/D_{bulk} is a bit more complex as discussed by Garboczi et al. (1995). Because in these studies, due mainly to the smaller aggregate surface area of a concrete relative to that of a mortar, the ratio of D_{ITZ} to D_{bulk} is generally less than five, adding additional aggregates will, on the whole, result in a decrease in the value of D_{conc}/D_{bulk} (Garboczi et al. 1995).

Coarse Aggregate Particle Size Distribution—Changing the coarse aggregate particle size distribution from "fine" (Curve A in Fig. 2) to "coarse" (Curve B) lowers the volume of ITZ cement paste present in a given concrete due to the reduction in aggregate surface area. This in turn increases the *W/C* ratio of the bulk paste

and thus increases D_{bulk}, but only slightly for the distributions examined in this study. As the coarse aggregate PSD varies from fine to coarse, the ratio of D_{ITZ}/D_{bulk} decreases very slightly, and because there is also less ITZ cement paste, the ratio of D_{conc}/D_{bulk} decreases as well. These two effects tend to cancel each other out so that the overall influence of coarse aggregate PSD on concrete diffusivity is negligible within the range examined in this study.

Fine Aggregate Particle Size Distribution—The arguments introduced above for the coarse aggregate PSD also apply for the fine aggregate PSD, but even more so due to the increased surface area per unit volume of the fine aggregate. Once again, the overall effect is observed to be negligible.

Interfacial Transition Zone Thickness—Increasing the value of t_{ITZ} naturally increases the volume of ITZ cement paste. This in turn once again decreases the effective "bulk" *W/C* ratio, so that D_{bulk} is decreased. However, an increase in t_{ITZ} significantly increases both V_{ITZ} and D_{ITZ}/D_{bulk}, and thus increases D_{conc}/D_{bulk}. These two effects are in opposition to one another, with the latter dominant, so that the overall concrete diffusivity is only slightly increased due to the larger value of t_{ITZ}.

Air Content—Air voids should tend to mimic the effects described above for an increase in aggregate volume fraction, the main difference being their much smaller size and higher surface area per unit volume. Thus, while their addition does slightly decrease the value of D_{bulk}, due to the large amount of additional ITZ cement paste, the value of D_{conc}/D_{bulk} increases. The two effects are again competing and result in a small decrease in concrete diffusivity as the air content is increased from 0% to 10%.

Considering only the three most significant variables (*W/C* ratio, degree of hydration (α), and volume fraction of aggregate (V_{agg})), the following equation for computing chloride diffusivity of concrete has been estimated by ordinary least squares regression:

$$D\left(\frac{m^2}{s}\right) = 10^{(-10.22+8.58(W/C)-4.99\alpha-3.04V_{agg}+5.09\alpha(W/C)-0.91(W/C)V_{agg}+1.6\alpha V_{agg}-6.58(W/C)^2-0.92\alpha^2+0.53V_{agg}^2)} \quad (4)$$

The diffusion coefficients calculated according to this equation are compared to the actual computer simulation results in Fig. 4. In general, the predicted values are within a factor of 1.5 of the actual values as indicated by the upper and lower solid lines in Fig. 4, with a ratio of 2 being the worst case.

Figure 5 provides a contour plot for the log of the concrete diffusivity versus degree of hydration and *W/C* ratio at a fixed volume fraction of aggregate of 0.675. Because the slope of the isolevel lines is greater than 45°, one can infer that *W/C* ratio has a stronger influence on diffusivity than degree of hydration, except for very high values of chloride diffusivity. Two other points are worth noting on the figure. First, because for low *W/C* ratio concretes, there is a maximal achievable degree of hydration which is less than one (as the capillary porosity goes to a value of zero) (Mindess 1981), the upper-most isolevel line indicating a chloride diffusivity of $10^{-12.5}$ ($3.2 \cdot 10^{-13}$ m^2/s) can basically be considered as a lower bound for the chloride ion diffusivity of conventional concretes, according to the computer simulation results. For low *W/C* ratio cement pastes, the maximal achievable degree of hydration is typically given by (*W/C*)/0.4 or (*W/C*)/0.42, so that for a *W/C* ratio of 0.3, the maximum value would be on the order of 0.73, which corresponds quite closely to the upper-most isolevel diffusivity line. Thus, there is definitely a lower limit on the diffusivities achievable using conventional concrete mixture proportions and curing practices. Second, for higher *W/C* ratios, the effects of a change in *W/C* ratio on concrete diffusivity are much less marked, as indicated

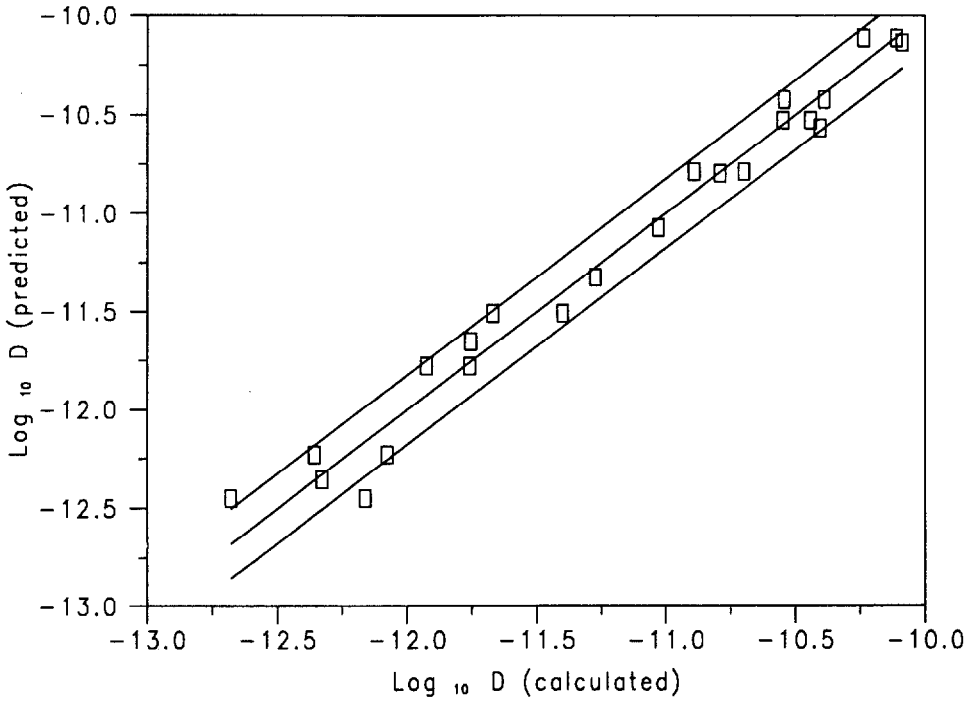

FIG. 4—*Comparison of predicted results based on Eq 4 with those from the computer experiment.*

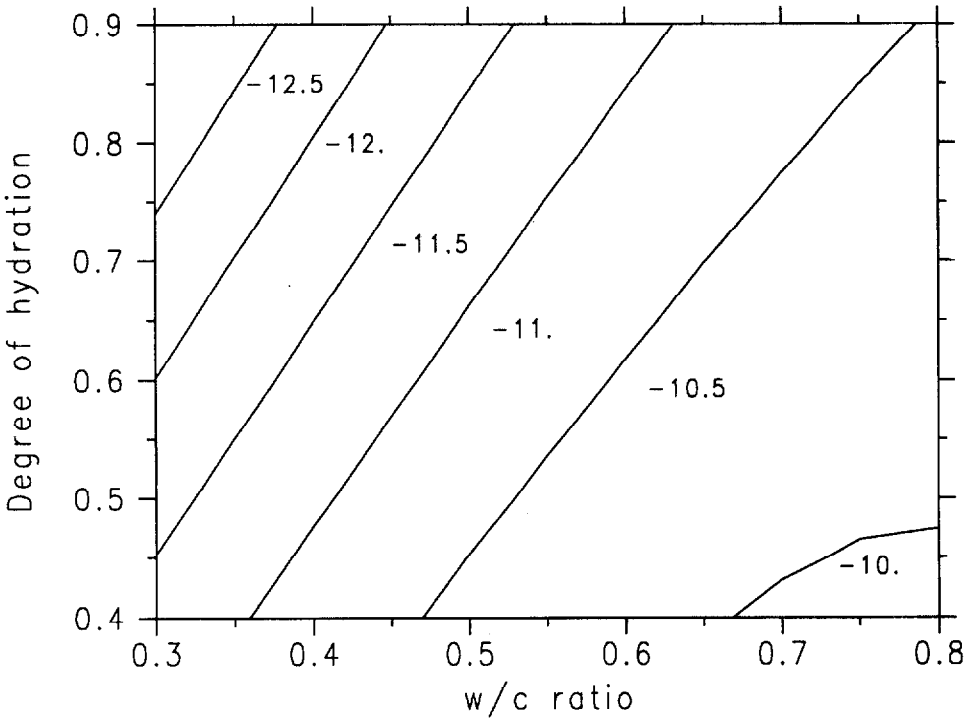

FIG. 5—*Contour plot for the $\log_{10}$ of concrete diffusivity versus* W/C *ratio and degree of hydration for a fixed volume fraction of aggregate of 0.675.*

by the greater distance between the -10.5 and -10 isolevel lines. Thus, only minimal hydration (<0.5) is needed to obtain a chloride diffusivity on the order of 10^{-10} m^2/s. Of course, it should be kept in mind that this value is only a factor of 20 below that of chloride ions in bulk water.

Equation 4 can be compared to that established by Walton et al. (1990) based on data compiled for chloride ion diffusion in cement paste by Atkinson et al. (1984):

$$D\left(\frac{m^2}{s}\right) = 10^{(6.0(W/C)-13.84)} \tag{5}$$

Figure 6 compares the equation of Walton et al. to Eq 4 with four sets of values for degree of hydration and volume fraction of aggregate. The curves for the lower volume fraction of aggregate fit well with Eq 5 for *W/C* ratios between 0.3 and 0.6, with significant deviations at higher *W/C* ratios. Thus, the equation derived here appears to be reasonable in terms of one previously determined with *W/C* ratio as the only variable. However, Eq 4 has the advantage of accounting for variability in degree of hydration and mixture proportions which should allow for a more accurate prediction of concrete chloride diffusivity.

Comparison to Published Diffusivity Values

There are few experimental data sets in the literature to which the results of the current computer simulation study can be compared. Tang and Nilsson (1992) do provide a set of measured chloride diffusion coefficients for concretes produced with *W/C* ratios of 0.32 and 0.7 at several different ages. The mixture proportions are also given so that the volume fraction of aggregate can be computed. While the age of the specimens at the times of test are given, no information is provided concerning the accompanying degrees of hydration. Thus, Eq 4 was used to determine the degrees of hydration that best fit the experimental diffusivity data. The results are summarized in Table 3. The estimated degrees of hydration for the two different *W/C* ratios are certainly plausible. Recent measurements on two cements mixed at a *W/C* ratio of 0.3 resulted in measured degrees of hydration of about 0.37, 0.53, 0.60, and 0.66 at 1, 3, 7, and 28 days, respectively (Bentz 1995). While the 1-day value is in good agreement with that predicted by Eq 4, the predicted hydration at the intermediate ages is somewhat less than these measured values. Of course, some variation will be observed due to the different particle size distributions and phase distributions of the cements, as well as the mixing conditions employed (Bentz 1995). Regarding the long-term hydration values, Waller et al. (1996) have recently proposed an equation for the long-term degree of hydration α_c as a function of *W/C* ratio of the form:

$$\alpha_c = 1.0 - \exp\left(-3.15 \cdot \frac{W}{C}\right) \tag{6}$$

Equation 6 predicts long-term degrees of hydration of 0.635 and 0.89 for *W/C* ratios of 0.32 and 0.7, respectively, once again in reasonable agreement with the values estimated for the greatest ages in Table 3, based on fitting Eq 4 to the measured diffusion data. Because *W/C* ratio is the only variable in Eq 5, it can be directly applied to estimating diffusivities for the two concretes. Thus, a diffusivity of $2.3 \cdot 10^{-10}$ m^2/s is predicted for a *W/C* ratio of 0.7, approximately one order of magnitude higher than the experimentally observed 7 to 90 day values. The value predicted by Eq 5 for a *W/C* ratio of 0.32, $1.2 \cdot 10^{-12}$ m^2/s, is in reasonable agreement with the measured long-term values in Table 3.

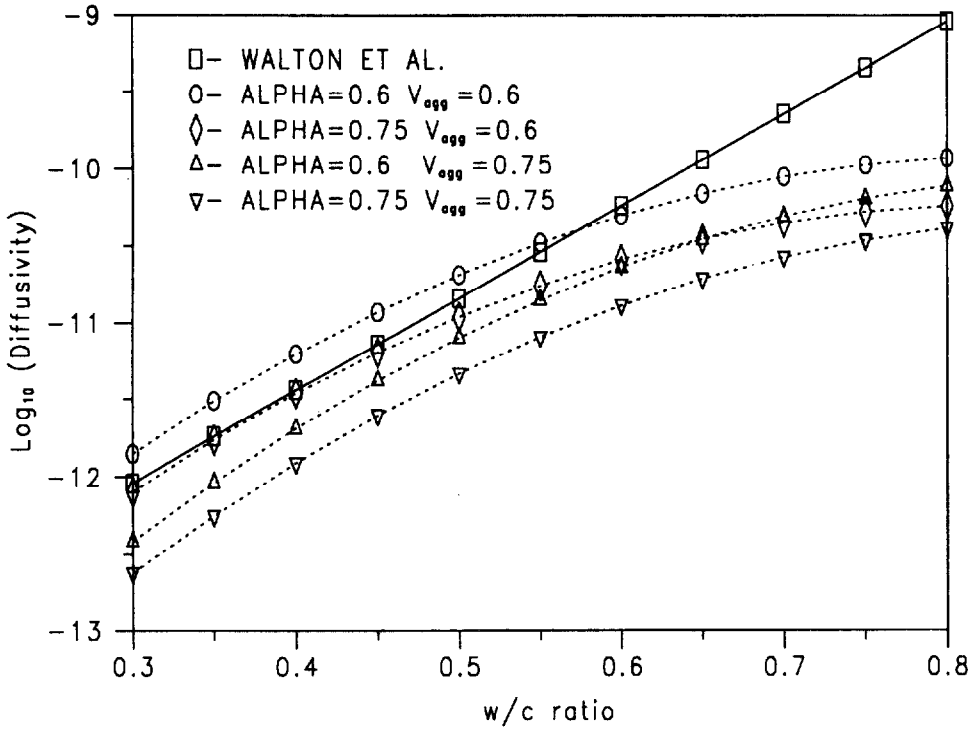

FIG. 6—*Comparison of current results to those of Walton et al. for diffusivity versus* W/C *ratio.*

TABLE 3—*Comparison of experimental (Tang and Nilsson 1992) and model data.*

W/C, mass	V_{agg}	*D* (10^{-12} m^2/s)	Curing Age, *d*	Computed, α
0.32	0.66	7.39	1	0.38
0.32	0.66	6.22	3	0.41
0.32	0.66	4.93	7	0.44
0.32	0.66	3.22	28	0.5
0.32	0.66	1.79	90	0.58
0.32	0.66	1.74	180	0.58
0.7	0.725	45.6	1	0.62
0.7	0.725	26.95	3	0.77
0.7	0.725	21.1	7	0.83
0.7	0.725	14.5	28	0.92
0.7	0.725	15.3	90	0.91

Assessment of Surface Effects

A secondary issue requiring consideration when assessing the diffusion and hydration properties of a concrete is the difference in volume proportions of the surface layer of the concrete. Because of the placement and finishing, the top surface of the concrete will most likely contain a higher volume fraction of cement paste and less coarse aggregate than the bulk of the concrete. The concrete microstructure model described previously can also be used to investigate the likely extent of this surface layer, in a manner similar to that previously illustrated by Wittmann et al. (1984–1985). To do this using the model, the aggregates are allowed to extend freely beyond all faces of the three-dimensional concrete volume, except for the top surface. At the top surface, aggregates which, when placed randomly, protrude through the top surface of the concrete volume are directly lowered until their highest point is just even with the top surface of the concrete, a crude approximation of the finishing process. If this new placement location would cause an overlap with an already placed aggregate, a new random location is chosen and the placement re-evaluated.

Using these techniques and a particle size distribution for a uniform blend of aggregates provided in Shilstone (1990), five random configurations of a concrete 3 · 3 · 6 cm with a 65% volume fraction of aggregate were generated. Figure 7 shows a density distribution for the aggregates in one 3 · 3 · 6 cm volume of concrete, with brightness indicating the aggregate density through the volume of the specimen perpendicular to one of its faces. The dark quarter circle at the upper right edge is ¼ of a rebar and one can clearly see the lower aggregate contents (darker regions) at the free concrete surface (left edge) and immediately surrounding the rebar. Based on these five random configurations, systematic point sampling was used to determine the average volume fraction of aggregate in the concrete, **excluding the rebar**, as a function of distance from the top surface of the concrete as shown in Fig. 8. For this particular size distribution of aggregates, it seems that the surface layer extends to a depth of about 5 mm, in good agreement with the experimental measurements of Crumbie et al. (1989), and in reasonable agreement with the 10 mm presented in Wittmann et al. (1984–1985). Thus, when analyzing specimens obtained from within the first 5 to 10 mm of depth of the concrete, one must remember that the aggregate volume fraction is significantly lower than in the bulk concrete. Because of the higher paste content in this surface layer, for instance, one would expect to measure a higher content of chlorides than immediately below the surface layer, which often causes problems when trying to interpret chloride penetration profiles based on a simple application of Fick's second law. Strength, water absorption, and shrinkage would also be expected to vary with distance from the surface due to this spatial variability of aggregate content (Wittmann et al. 1984–1985).

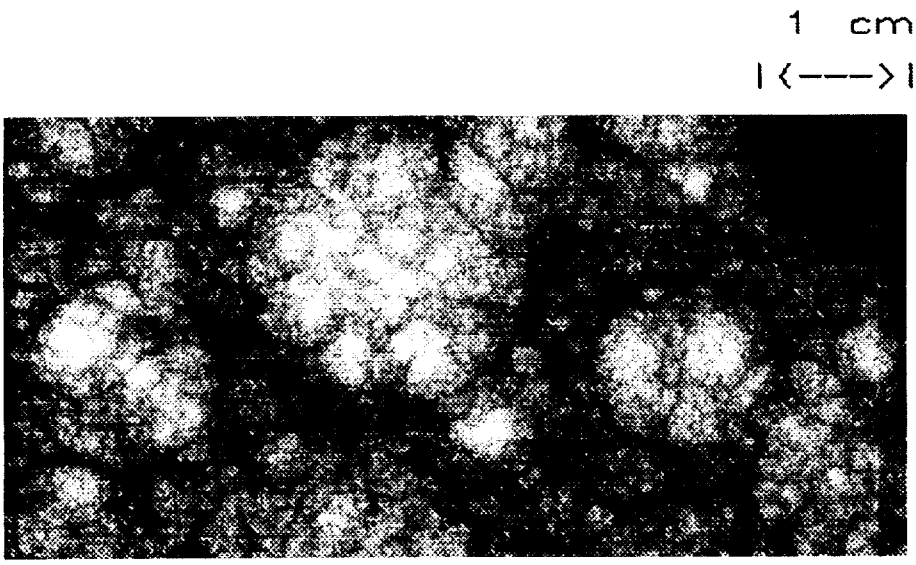

FIG. 7—*Spatial variation in aggregate density for a volume of concrete 3 · 3 · 6 cm in size.*

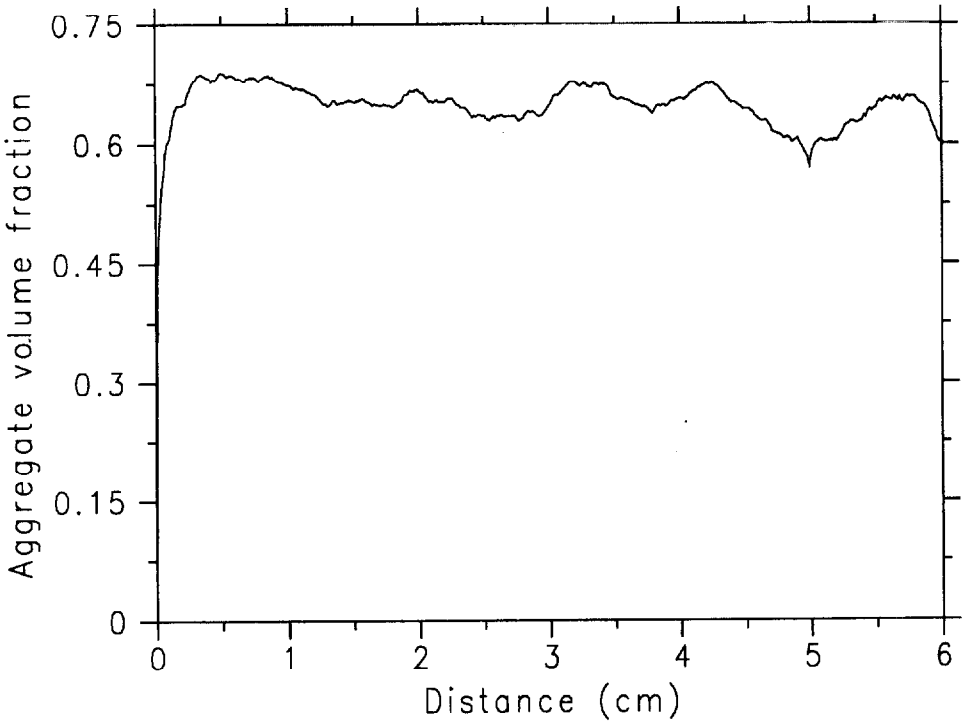

FIG. 8—*Simulated aggregate distribution in concrete with rebar centered at a depth of 6 cm.*

Discussion and Summary

The exercise in Section 4.2 should in no way be considered to be a validation of the computer model presented here. It will be necessary for a complete set of experimental measurements to be obtained, including measurement of the degree of hydration of the concrete at the age at which its chloride diffusivity is measured, before Eq 4 can be applied with confidence. However, the overall results are encouraging enough to suggest that the trends indicated by the regression equation are indeed likely to be observed experimentally. The computer study has suggested that the three key variables necessary to predict diffusivity are *W/C* ratio, degree of hydration, and volume fraction of aggregate. In addition, the influence of interfacial transition zone thickness and air content may warrant further experimental study.

The assumption of spherical-shaped aggregates is probably not a critical parameter for the following reason. While computer simulations have shown that ellipsoidal-shaped aggregates can significantly increase the volume of ITZ cement paste in a concrete (Bentz et al. 1995b), the present study has shown that this effect is offset by the concurrent reduction in the *W/C* ratio of the bulk cement

paste. Thus, while aggregate surface area and V_{ITZ} were strongly influenced by the coarse and fine aggregate particle size distributions, these variables had practically no influence on the final resultant diffusivities of the model concretes.

It should also be pointed out that all of the results generated in this study are for a portland cement concrete and do not consider the addition of pozzolans such as silica fume and fly ash. Previous computer simulation (Bentz and Garboczi 1991b) and experimental studies (Scrivener et al. 1988; Cohen et al. 1994) have clearly shown that these pozzolans can greatly modify the interfacial transition zone microstructure in concrete. In addition, most diffusivity studies indicate that these pozzolanic materials also have a marked influence on the diffusion properties of concretes, and thus, their presence would almost certainly warrant the addition of another term (perhaps the ratio of pozzolan addition to cement, *S/C*) to the developed diffusivity equation. The presence of these materials also complicates the measurement of degree of hydration by nonevaporable water content (Yogendran et al. 1991; Zhang and Gjorv 1991), so that heat release measurements or a combination of analytical techniques (Atlassi 1993) including image analysis of microstructural images, may be needed to gage the progress of the hydration and pozzolanic reactions.

Once validated, Eq 4 could be incorporated into a durability-based design specification to predict the expected service life of a reinforced concrete exposed to an external chloride environment (Clifton and Knab 1989; Bentz et al. 1996). Current mixture proportioning practices generally consider only slump and compressive strength as performance parameters, with the additional specification of air entrainment, when necessary. Using the models developed here should allow the extension of these practices to also consider a priori the durability of the concrete in a chloride environment, perhaps as a supplement to the recently proposed performance criteria for highway concretes (Goodspeed et al. 1996).

In summary, a computer experiment has been conducted to investigate the effects of mix parameters and curing on the chloride ion diffusivity of concrete. A set of multi-scale microstructural models has been used to quantitatively predict chloride diffusivity given the complete mixture proportions and projected degree of hydration of a concrete. Via this analysis, *W/C* ratio, degree of hydration, and volume fraction of aggregate have been identified as the three major variables affecting diffusion coefficients. An equation has been developed to quantitatively predict diffusion coefficients based on these three variables. While few data sets currently exist in the literature where the three key variables have been quantified and diffusion coefficients measured, previously developed equations and data where age is available as opposed to degree of hydration both provide reasonable agreement with the newly developed equation. Further simulations have been conducted to provide insight into the extent of the surface layer effect. It is strongly recommended that future experimental studies of chloride ion diffusivity also include measurements of degree of hydration and quantitative reporting of the employed mixture proportions so that the regression coefficients determined in this computer study may be modified to best represent field concrete.

Acknowledgments

The authors would like to thank Kenneth Snyder of BFRL (NIST) and Dr. James Filliben of ITL (NIST) for several useful discussions during the course of this research. We would also like to acknowledge the National Science Foundation Science and Technology Center for Advanced Cement-Based Materials for partial funding of this research.

References

Annual Book of ASTM Standards, 1995, Concrete and Aggregates, Vol. 04. 02, American Society for Testing and Materials, West Conshohocken, PA.

Atkinson, A. and Nickerson, A. K., 1984, *Journal of Materials Science,* Vol. 19, pp. 3068–3078.

Atkinson, A., Nickerson, A. K., and Valentine, T. M., 1984, "The Mechanism of Leaching from some Cement-Based Nuclear Wasteforms," *Radioactive Waste Management and the Nuclear Fuel Cycle,* Vol. 4, No. 4, pp. 357–378.

Atlassi, E. H., 1993, "A Quantitative Thermogravimetric Study on the Nonevaporable Water in Mature Silica Fume Concrete," Ph.D. Thesis, Chalmers University of Technology, Goteburg, Sweden.

Basheer, P. A. M., Henderson, G. D., and Long, A. E., 1996, "Proportioning Normal Concrete Mixtures for Durability," submitted to *Concrete International.*

Bentz, D. P. and Garboczi, E. J., 1991a, *Cement and Concrete Research,* Vol. 21, pp. 325–344.

Bentz, D. P. and Garboczi, E. J., 1991b, *ACI Materials Journal,* Vol. 88, No. 5, pp. 518–529.

Bentz, D. P. and Garboczi, E. J., 1992a, "Guide to Using HYDRA3D: A Three-Dimensional Digital-Image-Based Cement Microstructural Model," NISTIR 4746 U.S. Department of Commerce.

Bentz, D. P., Garboczi, E. J., and Stutzman, P. E., 1992b, "Computer Modeling of the Interfacial Zone in Concrete," in *Interfaces in Cementitious Composites,* J. C. Maso, Ed., Vol. 18, pp. 107–116.

Bentz, D. P., Coveney, P., Garboczi, E. J., Kleyn, M., and Stutzman, P. E., 1994, *Modelling and Simulation in Materials Science and Engineering,* Vol. 2, No. 4, pp. 783–808.

Bentz, D. P., 1995, "A Three-Dimensional Cement Hydration and Microstructure Program. I. Hydration Rate, Heat of Hydration, and Chemical Shrinkage," NISTIR 5756, U.S. Department of Commerce, and the many references provided therein.

Bentz, D. P., Quenard, D. A., Baroghel-Bouny, V., Garboczi, E. J., and Jennings, H. M., 1995a, *Materials and Structures,* Vol. 28, pp. 450–458.

Bentz, D. P., Hwang, J. T. G., Hagwood, C., Garboczi, E. J., Snyder, K. A., Buenfeld, N., and Scrivener, K. L., 1995b, "Interfacial Zone Percolation in Concrete: Effects of Interfacial Zone Thickness and Aggregate Shape," in *Microstructure of Cement-Based Systems/Bonding and Interfaces in Cementitious Materials,* MRS Symposium Proceedings, Vol. 370, pp. 437–442.

Bentz, D. P., Clifton, J. R., and Snyder, K. A., 1996, *Concrete International,* Vol. 18. No. 12, pp. 42–47.

Bentz, D. P., Detwiler, R. J., Garboczi, E. J., Halamickova, P., and Schwartz, L. M., 1997, "Multi-Scale Modelling of the Diffusivity of Mortar and Concrete," in *Chloride Penetration into Concrete,* L. O. Nilsson and J. P. Ollivier, Eds., RILEM, pp. 85–94.

Box, G. E. P., Hunter, W. G., and Hunter, J. S., 1978, *Statistics for Experimenters,* John Wiley and Sons, New York.

Clifton, J. R. and Knab, L. I., 1989, "Service Life of Concrete," NISTIR 89-4086 U.S. Department of Commerce.

Cohen, M. D., Goldman, A., and Chen, W. F., 1994, *Cement and Concrete Research,* Vol. 24, pp. 95–98.

Crumbie, A. K., Scrivener, K. L., and Pratt, P. L., 1989, "The Relationship Between the Porosity and Permeability of the Surface Layer of Concrete and the Ingress of Aggressive Ions," *Pore Structure and Permeability of Cementitious Materials,* MRS Symposium Proceedings, Vol. 137, pp. 279–284.

Garboczi, E. J. and Bentz, D. P., 1992, *Journal of Materials Science,* Vol. 27, pp. 2083–2092.

Garboczi, E. J., Schwartz, L. M., and Bentz, D. P., 1995, *Advanced Cement-Based Materials,* Vol. 2, pp. 169–181.

Gautefall, O., 1986, American Concrete Institute Special Publication 91-48, Madrid, pp. 991–997.

Goodspeed, C. H., Vanikar, S., and Cook, R. A., Feb. 1996, *Concrete International,* pp. 62–67.

Halamickova, P., Detwiler, R. D., Bentz, D. P., and Garboczi, E. J., 1995, *Cement and Concrete Research,* Vol. 25, No. 4, pp. 790–802.

Hooton, R. D., 1995, "Some Limitations of Our Existing Standards," *Cement, Concrete, and Aggregates,* Vol. 17, No. 2.

Mills, R. and Lobo, V. M. M., 1989, *Self-Diffusion in Electrolyte Solutions,* Elsevier, Amsterdam, p. 317.

Mindess, S. and Young, J. F., 1981, *Concrete,* Prentice-Hall, Englewood Cliffs, NJ.

Neter, J., Wasserman, W., and Kutner, M. H., 1990, *Applied Linear Statistical Models* Irwin, Boston.

Page, C. L., Short, N. R., and El Tarras, A., 1981, *Cement and Concrete Research,* Vol. 11, No. 3, pp. 395–406.

Powers, T. C., 1959, *PCA Bulletin,* No. 10, pp. 2–12.

Rashed, A. I., and Williamson, R. B., 1991, *Journal of Materials Research,* Vol. 6, pp. 2004–2012.

Schwartz, L. M., Garboczi, E. J., and Bentz, D. P., 1995, *Journal of Applied Physics,* Vol. 78, pp. 5898–5908.

Scrivener, K. L., Bentur, A., and Pratt, P. L., 1988, *Advances in Cement Research,* Vol. 1, No. 4, pp. 230–237.

Shilstone, J. M., Sr., June 1990, *Concrete International,* pp. 33–39.

Snyder, K. A. and Clifton, J. R., 1994, "Measures of Air Void Spacing," *Proceedings,* International Conference on Building Materials: Volume 1, Weimar, Germany, pp. 155–158.

Tang, L. and Nilsson, L. O., 1992, "Chloride Diffusivity in High Strength Concrete at Different Ages," *Nordic Concrete Research,* No. 11 (1), pp. 162–171.

Van Breugel, K., 1991, "Simulation of Hydration and Formation of Structure in Hardening Cement-Based Materials," Ph.D. Thesis, Delft University of Technology, Delft, The Netherlands, p. 228.

Waller, V., DeLarrard, F., and Roussel, P., 1996, "Modelling the Temperature Rise in Massive HPC Structures," Paper 170, *4th International Symposium on Utilization of High-Strength/High-Performance Concrete,* RILEM, pp. 415–421.

Walton, J. C., Plansky, L. E., and Smith, R. W., 1990, "Models for Estimation of Service Life of Concrete Barriers in Low-Level Radioactive Waste Disposal," NUREG/CR-5542 EGG-2597.

Winslow, D. N. Cohen, M. D., Bentz, D. P., Snyder, K. A., and Garboczi, E. J., 1994, *Cement and Concrete Research,* Vol. 24, pp. 25–37.

Wittmann, F. H., Roelfstra, P. E., and Sadouki, H., 1984–85, *Materials Science and Engineering,* Vol. 68, pp. 239–248.

Yogendran, Y., Langan, B. W., and Ward, M. A., 1991, *Cement and Concrete Research,* Vol. 21, pp. 691–708.

Zhang, M. H. and Gjorv, O. E., 1991, *Cement and Concrete Research,* Vol. 21, pp. 800–808.